SINGLE-CRYSTAL SILICON ACTUATOR ARRAYS FOR MICRO MANIPULATION TASKS

Karl-Friedrich Böhringer Bruce Randall Donald Noel C. MacDonald
Robotics and Vision Laboratory School of Electrical Engineering and
Department of Computer Science Cornell Nanofabrication Facility
Cornell University, Ithaca, NY 14853

URL `http://www.cs.cornell.edu/Info/People/karl/MicroActuators`

ABSTRACT

Arrays of electrostatic MEMS actuators have been fabricated using a modified, multi-layer SCREAM (Single-Crystal Reactive Etching and Metallization) process. The devices consist of released, torsionally suspended grids with high aspect ratio single-crystal silicon (SCS) tips. They can be used to generate a force field for the manipulation of small, flat objects. Calculations and experiments show that the actuator array is strong enough to move macroscopic parts. An individual actuator can generate a force of approximately 10 μN and a displacement of 5 μm. Monolithic arrays have been built reaching a size of up to 10 cm^2, with up to 15,000 individual single-crystal silicon actuators on one chip.

We investigate micro actuators for manipulation tasks, and discuss important issues and trade-offs in design, processing and fabrication. We describe manipulation experiments in which small, flat objects where lifted and moved. We conclude with an outlook on applications of programmable actuator arrays to more elaborate micro manipulation tasks and give an outline on how they can be used for transporting, positioning, sorting, and assembly of small parts.

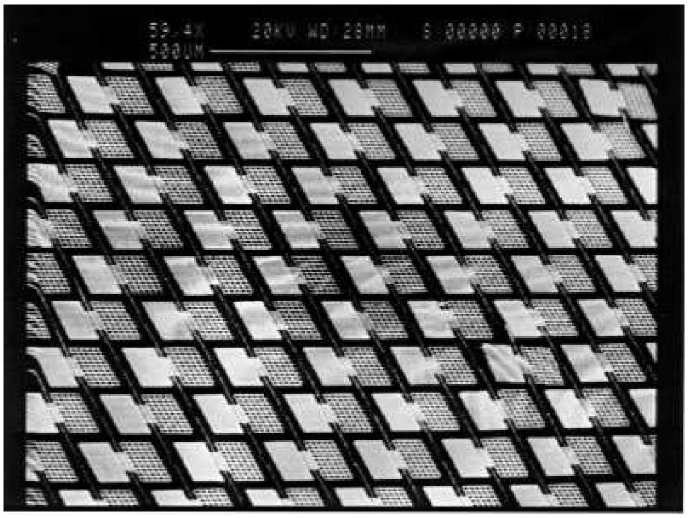

Figure 1: Large unidirectional actuator array (scanning electron microscopy). Each actuator is 180 $\times$ 240 μm^2 in size. Detail from a 10 cm^2 array with more than 15,000 actuators. For more pictures on device design and fabrication see URL `http://www.cs.cornell.edu/Info/People/karl/MicroActuators`.

INTRODUCTION

We investigate MEMS actuator arrays for micro manipulation tasks. There is a large potential of possible applications. Such actuator arrays can be used for automated parts positioning under a microscope, or as bulk-fabricated (cheap), ultra-thin transport mechanisms, e.g. for paper in copy machines or printers. At the other end of the spectrum, recent advances have brought within reach arrays equipped with tips that can probe and move objects consisting of only a few atoms [15]. Such devices, employed in a massively parallel fashion, will yield tremendous data storage capacities.

The MEMS array that we present here is designed for "medium size" applications in which objects in the millimeter range are moved, e.g. for a programmable stage of a microscope, or for the automated handling and assembly of small parts.

A wide variety of actuation principles for micro manipulation systems have been proposed in recent years. Pister et al. [10] presented a levitation system consisting of microfabricated nozzles, and electrostatic actuation. Konishi and Fujita [6] use controlled, directed micro air valves to convey small objects. Ataka et al. [1] simulate cilia with thermal bimorph micro structures. Liu et al. [7] propose a micro assembly system based on magnetic actuator arrays. Electrostatic actuator arrays are described by Böhringer et al. [5] and Storment et al. [14].

An important issue are the device design trade-offs between range of motion, strength, speed (actuation frequency), power consumption, control accuracy, system reliability and robustness. For example, thermal and magnetic actuators exhibit relatively large forces and displacements, but rely on significant currents, which in turn require high power input and cooling. Low power is sufficient for electrostatic actuators, which usually have a smaller range of motion.

Proc. IEEE Workshop on Micro Electro Mechanical Structures (MEMS), San Diego, CA, February 1996.

Compatibility with standard VLSI processes allows integration of control circuitry on the same chip. This is of great importance if we want to employ powerful manipulation strategies that require individual control of the actuators in the array. SCREAM is a low temperature process that can be performed after the fabrication of circuits. In the following sections we will discuss design, fabrication, and testing of a SCREAM electrostatic actuator array (see Figure 1).

FEASIBILITY AND DESIGN

Feasibility Calculations. To answer the question *Can microscopic actuators move macroscopic parts?* we consider the specific weight (i.e. the weight per area ratio) of a variety of objects and materials. For example, the specific weight of paper is approximately 1 $N/m^2 = 1\ \mu N/mm^2$. A silicon wafer is about ten times heavier at 10 $\mu N/mm^2$. We compare these values with the electrostatic force generated by a parallel-plate capacitor. The force per area ratio can be computed as $F/A = \varepsilon_0 V^2/d^2$, where V is the applied voltage, d is the gap width between the capacitor plates, and ε_0 is the permittivity of free space. For a gap width of 5 μm and a voltage of 60 V (typical values for our actuators), we obtain a value of approximately 1.2 mN/mm^2. This result is more than two orders of magnitude higher than the specific weight of a silicon wafer. This large margin is useful because we expect that design, layout, and fabrication constraints will reduce the effective generated force by approximately a factor 10, as is described in the following paragraphs.

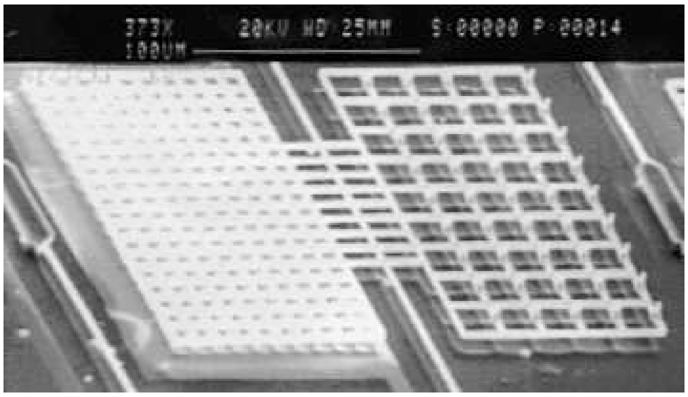

Figure 2: Released asymmetric actuator (scanning electron microscopy). Left: Dense grid (10 μm spacing) with aluminum electrode underneath. Right: Grid with 5 μm high poles.

SCS Torsional Actuator Design. A torsional actuator consists of a rectangular grid etched out of single-crystal silicon suspended by two rods that act as torsional springs (Figure 2). The design is based on torsional resonators [9]. In our current design, the grid is 180 μm long and extends 120 μm on each side of the rod. The rods are 150 μm long. The current asymmetric design has $5-10$ μm high protruding tips (Figure 3) on one side of the grid that make contact with an object lying on top of the actuator. The other side of the grid consists of more densely spaced beams above an aluminum electrode. If a voltage is applied between grid and electrode, the half of the grid above the electrode is pulled downward by the resulting electrostatic force. Simultaneously the other side of the grid (with the tips) is deflected out of the plane by several μm. Hence an object can be lifted and pushed sideways by the actuator.

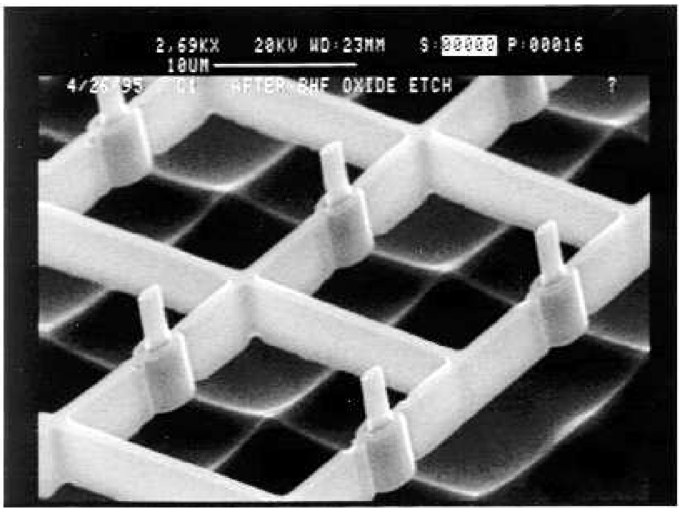

Figure 3: Released actuators consisting of single-crystal silicon with 5 μm high tips.

Because of its low inertia (resonance in the high kHz range) the device can be driven in a wide frequency range from DC to several 100 kHz AC. Due to the asymmetry in the actuator design, each actuator generates motion in one specific direction if it is activated; otherwise it acts as a passive frictional contact. Figure 1 shows a small portion of such a unidirectional actuator array, which consists of more than 15,000 individual actuators that densely cover the substrate surface.

The layout of the array can be changed such that the actuators point in various orientations. Then the combination and selective activation of several actuators in different orientations (*motion pixels*) allows us to generate various motions in discrete directions, spanning the plane.

Device Analysis. Actuation is based on the torsional out-of-plane deflection of an individual device. This angular deflection θ is limited by the gap height g between actuator grid and trench bottom electrode, such that $\sin\theta = g/l$, where l is the width of the actuator. In the current design $l = 120$ μm and $g = 5$ μm, hence $\theta \approx 2.4°$. Simultaneously there is a horizontal displacement which can be approximated by $(1-\cos\theta)\, l \approx 100$ nm. Several effects can contribute to the force transfer between actuator and object, in particular (sliding) frictional contact, dynamic impacts, or kinematic constraints due to surface roughness. If we assume motion induced solely by kinematic constraints, the object is moved in 100 nm steps each time the actuator is deflected. When operated at a frequency of 100 kHz, this corresponds to a velocity of 1 cm/sec. Depending on surface properties like roughness or elasticity, the speed of the object can be influenced by slip, deformation, and damping. More experiments will be necessary to determine the effects of these phenomena. But see e.g. [12, 11] for an investigation of friction in micro structures.

Design and layout constraints reduce the theoretically achievable electrostatic force. In the current array layout, only 30 percent of the densely packed chip surface can be used for electrostatic capacitors (see Figures 1 and 2).

Due to fabrication constraints for releasing SCREAM structures, the capacitor consists of a dense grid of beams rather than a plate. This reduces the effective capacity to about one-third, as determined by an FEM analysis. However, by using high aspect ratio vertical structures similar to comb drives it is possible to increase the effective surface area by a significant factor. These new designs are currently under investigation.

FABRICATION PROCESS

We use a modified SCREAM process to fabricate our devices. The original SCREAM (Single-Crystal Reactive Etching and Metallization) process [16, 13] is a single mask, reactive ion etching process for the fabrication of submicron, movable single-crystal silicon electromechanical structures. Recently, several process variations have been developed to create a wide variety of SCS MEMS devices, e.g. an integrated STM (scanning tunneling microscope), optoelectronic devices, and actuators in the milli-Newton range (see [8] for an overview). Characteristics of the SCREAM process are high aspect ratio SCS structures, high vertical stiffness, low in-plane and torsional stiffness, and compatibility with regular VLSI processes.

The layout of the complete devices comprising of torsional actuators with tips, electrodes, and contact pads was drawn using SYMBAD, a CAD package for IC (and MEMS) devices. The process flow for releasing an actuator beam with tips is shown in cross section in Figures 4 and 5.

On the substrate of an arsenic-doped, 0.005 Ωcm, n-type (100) silicon wafer, a 3.2 μm thick etch mask layer of silicon dioxide is deposited using plasma enhanced chemical vapor deposition at 300° C, 450 mT, N_2O flow of 42 sccm and SiH_4 flow of 12 sccm for 90 min. Photolithography is used to transfer the pattern of the tips from the mask onto a layer of KTI 985i 50cs positive resist spun on the oxide. The minimum feature size in our devices is 0.8 μm wide tips and beams. The pattern is transferred from the resist layer to the oxide layer using MRC Magnetron ion etching at 2 mT at a flow rate of 30 sccm of CHF_3 at 1000 W. The photo resist is removed using an O_2 plasma etch. The pattern is transferred into the silicon substrate from the silicon oxide

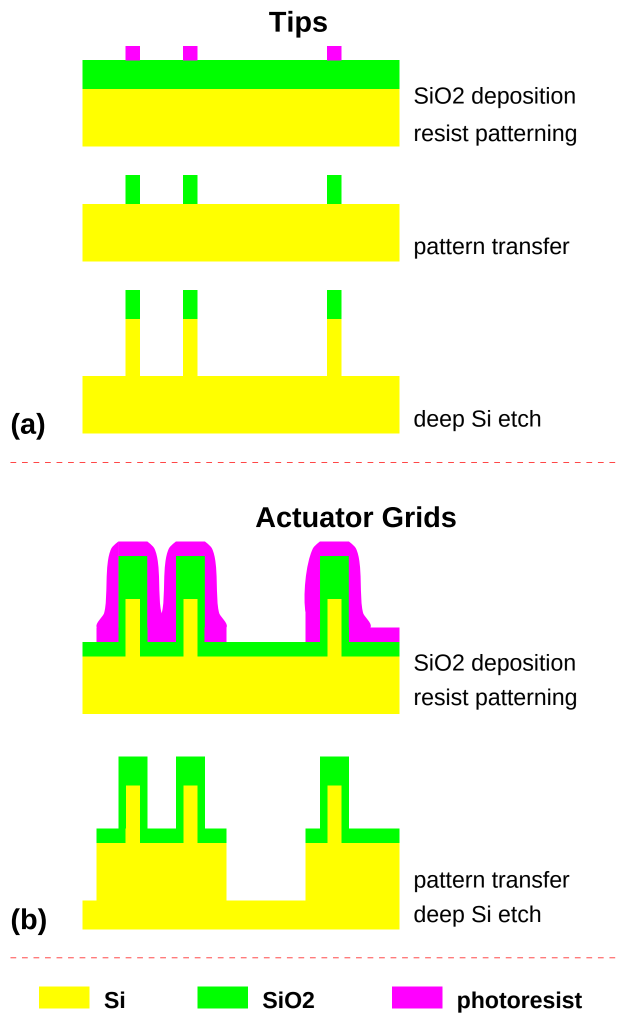

Figure 4: Device fabrication with a modified SCREAM process: (a) forming of tips using an RIE chlorine etch, (b) fabrication of actuator sructures consisting of SCS beams of 1 μm width.

layer using Cl_2 reactive ion etching in a Plasma Therm PK-1250 at 40 mT, 400 V and at a flow rate of 50 sccm for Cl_2 and 1.3 sccm BCl_3 for 30 min to get 5.0 μm deep trenches. This trench depth determines the height of the tips (see Figure 4a).

Then a 2.0 μm layer of mask SiO_2 is deposited, and the above steps are repeated for patterning of the actuator grids (Figure4b). This step requires careful characterization because lithography is performed on a non-flat surface.

Following this an insulating layer of silicon dioxide is deposited for side wall passivation using PECVD at the parameter values stated above for 15 min giving a 400 nm thick oxide layer (Figure 5c). CHF_3 reactive ion etching is again used to remove the floor oxide for subsequent substrate etches.

A short Cl_2 reactive ion etch at 50 sccm Cl_2 and 5 sccm BCl_3, 40 mT and 400 V for 10 min generates 2 μm deep trenches in the substrate to aid in the following release etch. All the beams of thickness up to 2 μm are released from the silicon substrate using an SF_6 RIE process in a Plasma Therm 72 RIE system. An SF_6 plasma with a flow rate of 140 sccm at 90 mT and 150 W is used to release the beams in 6 min. A 200 nm thin layer of dielectric silicon oxide is deposited. A 250 nm layer of Al is conformally deposited using DC magnetron sputtering performed at 30 mT pressure, with a beam current of 5 A and an Argon flow rate of 30 sccm. Due to overhanging sidewalls (see Figure 5d) trench and mesa are electrically isolated. Note however that the electrodes under the capacitor grids consist of continuous Aluminum. To pattern the Aluminum in the trench we use lithography with thin KTI 985i 5cs positive resist. The pattern is transferred using Cl_2 reactive ion etching in a Plasma Therm PK-1250 at 20 mT, 400 V, and flow rates of 20 sccm Cl_2, 40 sccm BCl_3, and 1.3 sccm CH_4 for 1.5 min.

A 100 nm thick layer of oxide is finally deposited on the device to avoid shorting when the actuators make contact with the trench electrodes during operation. The actuators consist of beams that are close to 1 μm wide and 5 μm high, with approximately 5 μm clearance underneath. Our current actuator designs have grids of $120 - 240$ μm side length. The fabrication can be done in less than one week in the Cornell Nanofabrication Facility (CNF) at Cornell University.

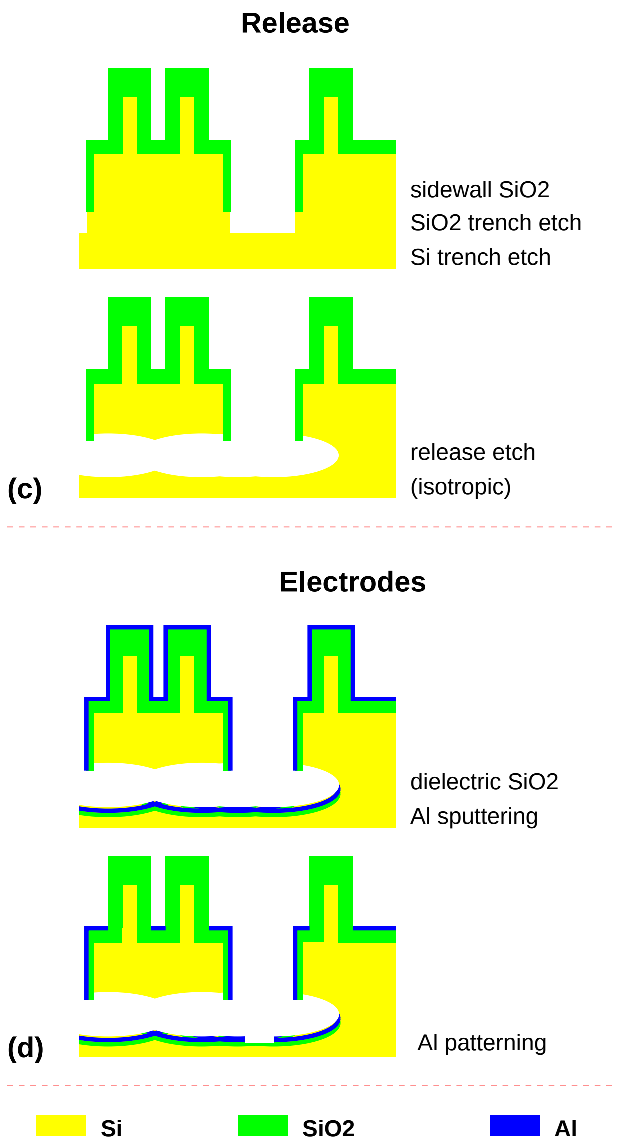

Figure 5: Device fabrication with modified SCREAM process: (c) MIE/RIE trench bottom etch and RIE release etch, (d) Aluminum electrode deposition and patterning.

EXPERIMENTS

Manipulation experiments were performed on a prototype array with more than 15,000 individual actuators. Each actuator measures approximately 0.1 μg in mass. The first set of manipulation experiments was performed with small glass pieces (microscope cover slips) of a few mm^2 size and close to 1 mg mass. We chose glass because it is flat, rigid, and transparent, which makes it a favorable material to test our devices. However, because of its smooth surface, the motion generated from the actuator array may be reduced because of slip between actuators and object.

We observed lifting of the glass pieces within the motion range of the actuators (several μm). The objects were also pushed sideways by several 100 μm. Larger distances were difficult to achieve with the current arrays because of the low yield of our prototype device. Depending on the shape of the object as well as its position on the actuator array, we also observed resonance between actuators and object at certain actuation frequencies.

A second round of experiments was performed with pieces of paper. Paper is considerably rougher and lighter than a glass piece of equal size. With the current actuator array no motion could be observed. We believe that the main reason for this result is the high surface roughness of paper which we measured at $10 - 100$ μm, which is in the same range as the height of our current actuators, and larger than their range of motion. Low yield in the current actuator arrays also reduces their effectiveness. Based on these experiments, an improved actuator array with higher tips, more out-of-plane motion, and higher yield is currently being built.

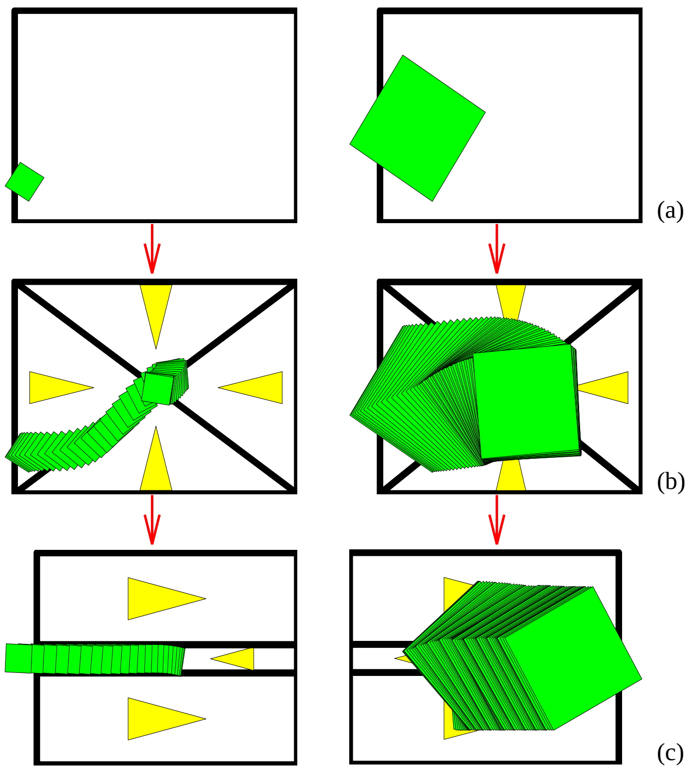

Figure 6: Sensorless sorting using force vector fields: Parts of various sizes are centered and subsequently separated depending on their size.

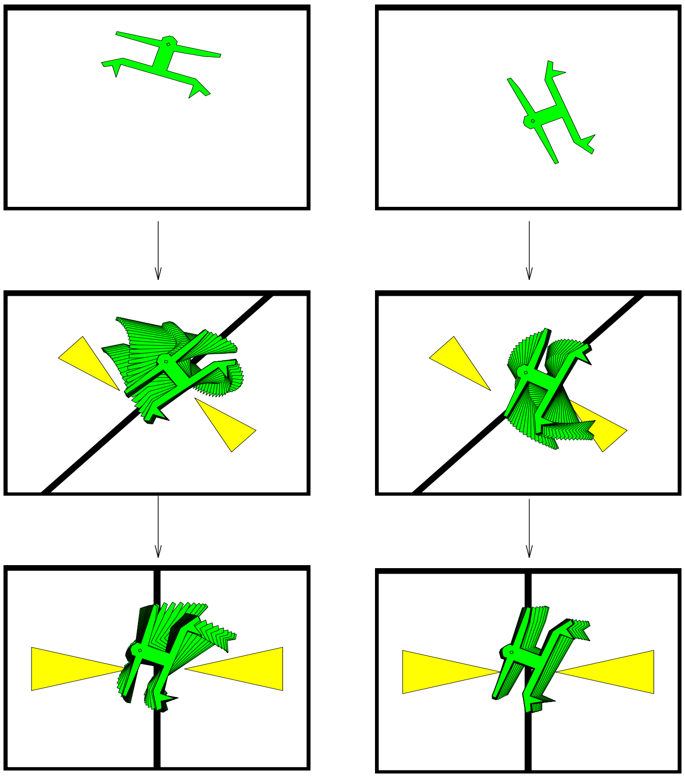

Figure 7: Sensorless alignment using force vector fields: Parts at arbitrary initial configurations are uniquely positioned by a sequence of force fields generated by a MEMS array. For an animated simulation see URL `http://www.cs.cornell.edu/Info/People/karl/MicroManipulation`.

SUMMARY AND FUTURE WORK

Electrostatic SCS Micro Actuator Arrays. We have presented a process for the fabrication of single-crystal silicon actuator arrays that are strong enough to perform useful manipulation tasks. The fabricated devices exhibit high aspect ratios, high vertical stiffness, and torsional deflection for out-of-plane motion. This process is low-temperature and compatible with traditional VLSI. Process extensions to integrate electronic circuitry next to or *in* the devices are possible. This opens the door for sophisticated actuator control strategies.

Manipulation Strategies. In earlier work we have presented several strategies for sorting, positioning, and orienting parts [5, 4]. The automatically generated manipulation plans are based on the principle of parts manipulation in *force vector fields* generated by MEMS arrays. These strategies are particularly interesting because they require no sensor input. Instead, we predict the stable equilibrium positions in which moving parts will settle by analyzing the force field that the actuators generate. It can be shown that for any part, in general there exist a small number of such equilibrium positions which can be determined algorithmically from the shape of the part. With a sequence of particular force fields, it is possible to further reduce the number of possible positions until a unique position is reached.

These strategies have been proven useful in theoretical analyses and simulations by various researchers [6, 5, 7]. For example consider Figure 6, where parts are first centered by a *radial centering field*. In a second step, small and large parts are sorted by a *separating field*. In Figure 7 a part is brought into a unique orientation with two *squeeze fields*. It has been shown [4] that the part always reaches this unique orientation independent of its initial position.

Modeling of Complex MEMS Systems. With a sufficiently powerful programmable actuator array, a wide range of force vector fields for parts manipulation can be generated. In recent work we have discussed several new algorithms for programmable force fields [2, 3] for centering, positioning, sorting, or assembly of small parts. Hence we are able to generate motion plans at a high (task) level and automatically transform them into an actuator array control strategy, in analogy to a compiler that translates high level instructions into assembler code. We believe that such high level strategies of micro sensors and actuators are essential for efficient control of future complex MEMS systems.

ACKNOWLEDGMENTS

This work was supported in part by the National Science Foundation under grants No. IRI-8802390, IRI-9000532, IRI-9201699, and by a Presidential Young Investigator award to Bruce Donald, in part by NSF/ARPA Special Grant for Experimental Research No. IRI-9403903, and in part by the Air Force Office of Sponsored Research, the Mathematical Sciences Institute, Intel Corporation, and AT&T Bell laboratories. Further support for this work was provided by ARPA under contract DABT 63-69-C-0019. The device fabrication was performed at the Cornell Nanofabrication Facility (CNF), which is supported by the NSF grant ECS-8619049, Cornell University, and Industrial Affiliates. We thank users, staff and students at the Cornell Nanofabrication Facility at Cornell University for their technical assistance.

REFERENCES

[1] M. Ataka, A. Omodaka, and H. Fujita. A biomimetic micro motion system. In *Transducers — Digest Int. Conf. on Solid-State Sensors and Actuators*, pages 38–41, Pacifico, Yokohama, Japan, June 1993.

[2] K.-F. Böhringer, B. R. Donald, and N. C. MacDonald. Classification and lower bounds for MEMS arrays and vibratory parts feeders: What programmable vector fields can (and cannot) do — Part I. Technical report, Cornell University, Robotics and Vision Laboratory, Ithaca, NY, Oct. 1995.

[3] K.-F. Böhringer, B. R. Donald, and N. C. MacDonald. New and improved manipulation algorithms for MEMS arrays and vibratory parts feeders: What programmable vector fields can (and cannot) do — Part II. Technical report, Cornell University, Robotics and Vision Laboratory, Ithaca, NY, Oct. 1995.

[4] K.-F. Böhringer, B. R. Donald, R. Mihailovich, and N. C. MacDonald. Sensorless manipulation using massively parallel microfabricated actuator arrays. In *Proc. IEEE Int. Conf. on Robotics and Automation (ICRA)*, pages 826–833, San Diego, CA, May 1994.

[5] K.-F. Böhringer, B. R. Donald, R. Mihailovich, and N. C. MacDonald. A theory of manipulation and control for microfabricated actuator arrays. In *Proc. IEEE Workshop on Micro Electro Mechanical Systems (MEMS)*, pages 102–107, Oiso, Japan, Jan. 1994.

[6] S. Konishi and H. Fujita. A conveyance system using air flow based on the concept of distributed micro motion systems. In *Transducers — Digest Int. Conf. on Solid-State Sensors and Actuators*, pages 28–31, Pacifico, Yokohama, Japan, June 1993.

[7] C. Liu, T. Tsao, P. Will, Y. Tai, and W. Liu. A micro-machined magnetic actuator array for micro-robotics assembly systems. In *Transducers — Digest Int. Conf. on Solid-State Sensors and Actuators*, Stockholm, Sweden, 1995.

[8] N. C. MacDonald, S. G. Adams, A. A. Ayon, K.-F. Böhringer, L.-Y. Chen, J. H. Das, D. Haronian, W. Hofmann, X. T. Huang, A. Jazairy, R. E. Mihailovich, S. A. Miller, I. Ogo, R. Prasad, B. W. Reed, M. T. A. Saif, K. A. Shaw, R. Y. Webb, and Y. Xu. Micromachined microdevices and microinstruments. In *Micro- And Nano-Engineering (MNE)*, Aix-en-Provence, France, Sept. 1995.

[9] R. E. Mihailovich, Z. L. Zhang, K. A. Shaw, and N. C. MacDonald. Single-crystal silicon torsional resonators. In *Proc. IEEE Workshop on Micro Electro Mechanical Systems (MEMS)*, pages 155–160, Fort Lauderdale, FL, Feb. 1993.

[10] K. S. J. Pister, R. Fearing, and R. Howe. A planar air levitated electrostatic actuator system. In *Proc. IEEE Workshop on Micro Electro Mechanical Systems (MEMS)*, pages 67–71, Napa Valley, California, Feb. 1990.

[11] R. Prasad, K.-F. Böhringer, and N. C. MacDonald. Design, fabrication, and characterization of SCS latching snap fasteners for micro assembly. In *Proceedings of the ASME International Mechanical Engineering Congress and Exposition (IMECE)*, San Francisco, California, Nov. 1995.

[12] R. Prasad, N. C. MacDonald, and D. Taylor. Micro-instrumentation for tribological measurements. In *Transducers — Digest Int. Conf. on Solid-State Sensors and Actuators*, Stockholm, Sweden, June 1995.

[13] K. A. Shaw, Z. L. Zhang, and N. C. MacDonald. SCREAM I: A single mask, single-crystal silicon process for microelectromechanical structures. In *Transducers — Digest Int. Conf. on Solid-State Sensors and Actuators*, Pacifico, Yokohama, Japan, June 1993.

[14] C. W. Storment, D. A. Borkholder, V. Westerlind, J. W. Suh, N. I. Maluf, and G. T. A. Kovacs. Flexible, dry-released process for aluminum electrostatic actuators. *Journal of Microelectromechanical Systems*, 3(3):90–96, Sept. 94.

[15] Y. Xu, S. A. Miller, and N. C. MacDonald. Microelectromechanical scanning tunneling microscope. *Bulletin of the American Physical Society*, 40(1):63, 1995.

[16] Z. L. Zhang and N. C. MacDonald. An RIE process for submicron, silicon electromechanical structures. *Journal of Micromechanics and Microengineering*, 2(1):31–38, Mar. 1992.